THE JOURNAL OF BIOLOGICAL CHEMISTRY VOL. 285, NO. 19, pp. 14122–14133, May 7, 2010
Printed in the U.S.A.

Schizosaccharomyces pombe Dss1p Is a DNA Damage Checkpoint Protein That Recruits Rad24p, Cdc25p, and Rae1p to DNA Double-strand Breaks*[S]

Received for publication, November 9, 2009, and in revised form, March 9, 2010 Published, JBC Papers in Press, March 15, 2010, DOI 10.1074/jbc.M109.083485

Saravana P. Selvanathan[‡], Anjan G. Thakurta[‡1], Jothy Dhakshnamoorthy[‡], Ming Zhou[§], Timothy D. Veenstra[§], and Ravi Dhar[‡2]

From the [‡]Basic Research Laboratory, Center for Cancer Research, NCI, National Institutes of Health, Bethesda, Maryland 20892 and the [§]Laboratory of Proteomics and Analytical Technologies, Advanced Technologies Program, Science Application International Corporation-Frederick, Inc., NCI, National Institutes of Health, Frederick, Maryland 21702

Schizosaccharomyces pombe **Dss1p and its homologs function in multiple cellular processes including recombinational repair of DNA and nuclear export of messenger RNA. We found that Tap-tagged Rad24p, a member of the 14-3-3 class of proteins, co-purified Dss1p along with mitotic activator Cdc25p, messenger RNA export/cell cycle factor Rae1p, 19 S proteasomal factors, and recombination protein Rhp51p (a Rad51p homolog). Using chromatin immunoprecipitation, we found that Dss1p recruited Rad24p and Rae1p to the double-strand break (DSB) sites. Furthermore, Cdc25p also recruited to the DSB site, and its recruitment was dependent on Dss1p, Rad24p, and the protein kinase Chk1p. Following DSB, all nuclear Cdc25p was found to be chromatin-associated. We found that Dss1p and Rae1p have a DNA damage checkpoint function, and upon treatment with UV light Δ*dss1* cells entered mitosis prematurely with indistinguishable timing from Δ*rad24* cells. Taken together, these results suggest that Dss1p plays a critical role in linking repair and checkpoint factors to damaged DNA sites by specifically recruiting Rad24p and Cdc25p to the DSBs. We suggest that the sequestration of Cdc25p to DNA damage sites could provide a mechanism for *S. pombe* cells to arrest at G_2/M boundary in response to DNA damage.**

Eukaryotic cells respond to double-strand breaks (DSBs)[3] within DNA by activating DNA damage checkpoint proteins that send signals to the cells, ultimately resulting in cell cycle arrest. The arrest allows DNA damage to be repaired by the proteins of the DNA repair pathway before cells can enter mitosis (1, 2). In *Schizosaccharomyces pombe*, entry into mitosis at the G_2/M boundary is regulated by the phosphorylation status of the mitotic regulator Cdc2p at the tyrosine 15 residue (3). The cells are maintained in G_2 by phosphorylation of Cdc2p by Wee1p and Mik1p kinases, whereas their entry into mitosis is triggered by dephosphorylation of Cdc2p by the Cdc25p phosphatase (3).

Dss1p, or its *Saccharomyces cerevisiae* homolog Sem1p, is a small acidic protein that is required for efficient DNA repair and the nuclear export of messenger RNA (mRNA) (4–7). Dss1p is a co-factor for human breast cancer susceptibility protein BRCA2 (8). In *Ustilago maydis*, a Dss1p homolog is a co-factor for Brh2p, a homolog of the human BRCA2 (9). The association between Dss1p and BRCA2 regulates the function of recombination-repair protein Rad51p (a homolog of the bacterial RecA; Rhp51p in *S. pombe*) (10, 11). So far the homologs of BRCA2/Brh2p have not been reported in either *S. cerevisiae* or in *S. pombe*. *S. cerevisiae* Sem1p was shown to recruit to DSB sites following a pattern similar to Rad51p, with high enrichment around the break site and gradually decreasing away from the break in both directions (12). Both Dss1p and Sem1p were shown to associate with the 19 S subunit of the 26 S proteasomes (12–14). It was suggested that the function of Sem1p involves regulating the function of the proteasome complex in DNA repair (12). So far the corresponding role of *S. pombe* Dss1p in DNA recombination-repair has not been studied.

S. pombe Rad24p belongs to the 14-3-3 family of proteins that play a significant role as checkpoint factors in monitoring DNA damage in the G_2 phase of the cell cycle (15–18). Their role in the cell cycle was first demonstrated in *S. pombe,* where the products of the *rad24* and *rad25* genes were shown to possess a DNA damage checkpoint function (19). Neither the *rad24* nor the *rad25* gene is essential for growth, but simultaneous loss of both genes is lethal (19). The loss of *rad24*, but not *rad25*, leads to premature entry of cells into mitosis, resulting in small, round cells. In addition, the loss of *rad24* renders cells highly sensitive to DNA-damaging agents, whereas a *rad25* null strain is only modestly sensitive (19). In response to DNA damage in the G_2 stage, activated Chk1p kinase phosphorylates Cdc25p. Recently Mek1p was shown to phosphorylate Cdc25p independent of Chk1p (20). Rad24p binds phosphorylated Cdc25p and apparently blocks a nuclear localization signal within Cdc25p. The Rad24p-Cdc25p complex exits the nucleus by using a dedicated nuclear export pathway. It was originally suggested that the "nuclear exclusion" of Cdc25p prevents the

* This work was supported, in whole or in part, by National Institutes of Health NCI intramural program.

[S] The on-line version of this article (available at http://www.jbc.org) contains supplemental Fig. 1S and Table 1S.

[1] Present address: AstraZeneca Pharmaceuticals, 1700 Auburn Ave., Rockville, MD 20850.

[2] To whom correspondence should be addressed: Basic Research Laboratory, Center for Cancer Research, NCI, National Institutes of Health, Bldg. 37, Rm. 5016, 37 Convent Dr., 9000 Rockville Pike, Bethesda, MD 20892. Tel.: 301-496-0990; Fax: 301-480-5088; E-mail: dharr@mail.nih.gov.

[3] The abbreviations used are: DSB, double-strand break; TAP, tandem affinity purification; GST, glutathione *S*-transferase; MMS, methyl methanesulfonate; HU, hydroxyurea; GFP, green fluorescent protein; ChIP, chromatin immunoprecipitation; mRNA, messenger RNA; HO, homothallic switching.

dephosphorylation and activation of the target of Cdc25p, Cdc2p, at tyrosine 15 (21). More recently, it has been shown that the exclusion of Cdc25p from the nucleus is not essential for inhibiting cell cycle progression (22).

S. pombe Rae1p is essential for the nuclear export of mRNA and functions in cell cycle progression from G_2 to M (23, 24). However, the role of Rae1p in the G_2/M transition was shown to be independent of its role in mRNA export (25). Thus far, no role for Rae1p has been implicated in DNA damage. A human homolog of Rae1p was found to be required in metaphase in mitotic spindle assembly. Through its interaction with the nuclear mitotic apparatus protein, human Rae1p is thought to be involved in bipolar spindle pole body formation (26–28). Whether *S. pombe* Rae1p plays a similar role remains to be investigated.

In this study, by using the tandem affinity purification (TAP) method, we found that Rad24p-TAP co-purified Dss1p and Rae1p. Several DNA repair proteins (for example, 19 S proteasomal subunits and Rhp51p) known to interact with Dss1p homologs also co-purified with the Rad24p-TAP fusion. By using an *S. pombe* strain carrying the *S. cerevisiae* homothallic switching (HO)endonuclease cleavage site and a plasmid expressing inducible HO-endonuclease (29), we conducted chromatin immunoprecipitation (ChIP) experiments to develop evidence that upon DNA damage, Dss1p mediates recruitment of DNA recombination/repair, cell cycle, and checkpoint control proteins to the DNA DSB sites. Finally, we found that Dss1p and Rae1p have a DNA checkpoint function, with Δ*dss1* cells timing of entry into mitosis indistinguishable from Δ*rad24* cells. Taken together, these results suggest that Dss1p plays a critical role in linking DNA repair and checkpoint factors to damaged sites by recruiting Rad24p and Cdc25p to the DNA DSB sites. We suggest that the recruitment of Cdc25p to the DSB site could lead to cell cycle arrest at the G_2/M boundary in *S. pombe* cells in response to DNA damage.

EXPERIMENTAL PROCEDURES

Strains and Culture—Basic genetic and cell culture techniques have been described previously (30, 31). The strains used in this study are described in Table 1. The *rad24-tap* strain was constructed by techniques described previously (32, 33), in which TAP is fused to the *rad24* gene at the C terminus by homologous recombination using the kanamycin gene as a selectable marker. Strains carrying the HO-endonuclease site were kind gifts from the laboratory of Paul Russell (The Scripps Research Institute, La Jolla, CA).

TAP Purification of Complexes—To identify mRNA export factors that may interact with Rad24p, an *S. pombe* strain expressing the Rad24p-TAP fusion protein from its chromosomal locus was used. As a control for these experiments, pNTAP41 was used. Purification of TAP-tagged proteins was performed by published methods using IgG-Sepharose beads (34). The complexes were cleaved from the beads by using TEV-protease. The cleaved fraction was next bound to calmodulin beads, and the bound proteins were eluted by calmodulin elution buffer and precipitated by trichloroacetic acid (34). Purified samples were separated on SDS-PAGE and visualized by Coomassie Blue staining, and associated proteins were identified using tandem mass spectrometry and/or Western blot analysis using specific antibodies (35, 36). The tandem mass spectrometry data were searched against the *S. pombe* data base from the Wellcome Trust Sanger Institute using BioWorks 3.3.1.

TABLE 1
***S. pombe* strains used in this study**

Genotypes	Source
h^- leu1-32 ura4-D18	Ref. 25
h^- leu1-32 ura4-D18 rae1-1	Ref. 23
h^- leu1-32 ura4-D18 ade6-704 rae1-1 rad24::ura4$^+$	This study
h^- leu1-32 ura4-D18 ade6-704 rad24::ura4$^+$	Ref. 19
h^- leu1-32 ura4-D18 rad24-TAP	This study
h^+ leu$^+$ ura4$^+$ rad1-1	Ref. 49
h^+ leu1-32 ura4-D18 ade$^-$ dss1::kan	Ref. 5
h^- leu1-32 ura4-D18 cdc25-GFPint cdc25::ura4$^+$	Ref. 50
h^- leu1-32::2xYFP-crb2$^+$ -leu1$^+$ ura4D18 crb2-D2::ura4$^+$ his3-D1 arg3::HO site-kanMX4	Ref. 29
h^- leu1-32::2xYFP-crb2$^+$ -leu1$^+$ ura4D18 crb2-D2::ura4$^+$ his3-D1 arg3::HO site-kanMX4 dss1::kan	This study
h^- leu1-32::2xYFP-crb2$^+$ -leu1$^+$ ura4D18 crb2-D2::ura4$^+$ his3-D1 arg3::HO site-kanMX4 rad24::ura4$^+$	This study
h^- leu1-32::2xYFP-crb2$^+$ -leu1$^+$ ura4D18 crb2-D2::ura4$^+$ his3-D1 arg3::HO site-kanMX4 cdc25-GFPint cdc25::ura4$^+$	This study
h^- leu1-32::2xYFP-crb2$^+$ -leu1$^+$ ura4D18 crb2-D2::ura4$^+$ his3-D1 arg3::HO site-kanMX4 cdc25-GFPint cdc25::ura4$^+$ rad24::ura4$^+$	This study
h^- leu1-32::2xYFP-crb2$^+$ -leu1$^+$ ura4D18 crb2-D2::ura4$^+$ his3-D1 arg3::HO site-kanMX4 cdc25-GFPint cdc25::ura4$^+$ chk1::ura4$^+$	This study

TABLE 2
Primers used in the ChIP experiments

Primer	Sequence
ChIP 1 (forward)	5′-TTTCATTGAGATAGACCACCT-3′
ChIP 1 (reverse)	5′-CTCTTTCTGTAGCTCGTAAAG-3′
ChIP 2 (forward)	5′-CCACCAACCTTGATAATAGCG-3′
ChIP 2 (reverse)	5′-GGCAATGCTTATTGAATTGCA-3′
ChIP 3 (forward)	5′-TGGCTGAAAATTACATCGGAAACC-3′
ChIP 3 (reverse)	5′-GAGAAGGGCTTCTTGCCAAAT-3′
ChIP 4 (forward)	5′-CATCCCTTTTCATTAGTTCTA-3′
ChIP 4 (reverse)	5′-GTCGACTACAAGGAACCCACA-3′
ChIP 5 (forward)	5′-CGCAGCTCAGGGGCATGATGT-3′
ChIP 5 (reverse)	5′-CTGATTGCCCGACATTATCGC-3′
ChIP 6 (forward)	5′-CTCTTCCGACCATCAAGCATT-3′
ChIP 6 (reverse)	5′-AATCACCATGAGTGACGACTG-3′
ChIP 7 (forward)	5′-AACTGCCTCGGTGAGTTTTCT-3′
ChIP 7 (reverse)	5′-CACATACGATTGACGCATGAT-3′
ChIP 8 (forward)	5′-CCTCTTAACTAGATATTTCAAGG-3′
ChIP 8 (reverse)	5′-AAGGAATTGGCGGAAGACAAG-3′
ChIP 9 (forward)	5′-GTAACCACAAAGGTAGTTTCT-3′
ChIP 9 (reverse)	5′-AGGGGCTCTAGAACTAATGAG-3′
Internal control (forward)	5′-CAACAGGAGCGCTATAATAA-3′
Internal control (reverse)	5′-CAGATAGCTTGGATAGATATG-3′

Western Blot Detection—Polyclonal antibodies to *S. pombe* mRNA export factors were made by expressing the proteins in *Escherichia coli* and injecting them into rabbits as previously described (5, 37, 38). Antibodies to *S. pombe* Rad24p and Rhp51p were made by expressing the full-length *rad24* and *rhp51* genes in pET14b. Polyclonal antibodies to *S. pombe* Mts2p were bought from Biomol Research La. Standard chemiluminescent methods (PerkinElmer Life Sciences) were used to detect the purified proteins.

ChIP Analysis—ChIP analysis was performed using published protocols (39, 40). Following cross-linking of proteins to DNA and precipitation by different antibodies, specific primer pairs were used to amplify segments of DNA fragments precipitated by the specific antibodies (Table 2). As a control for

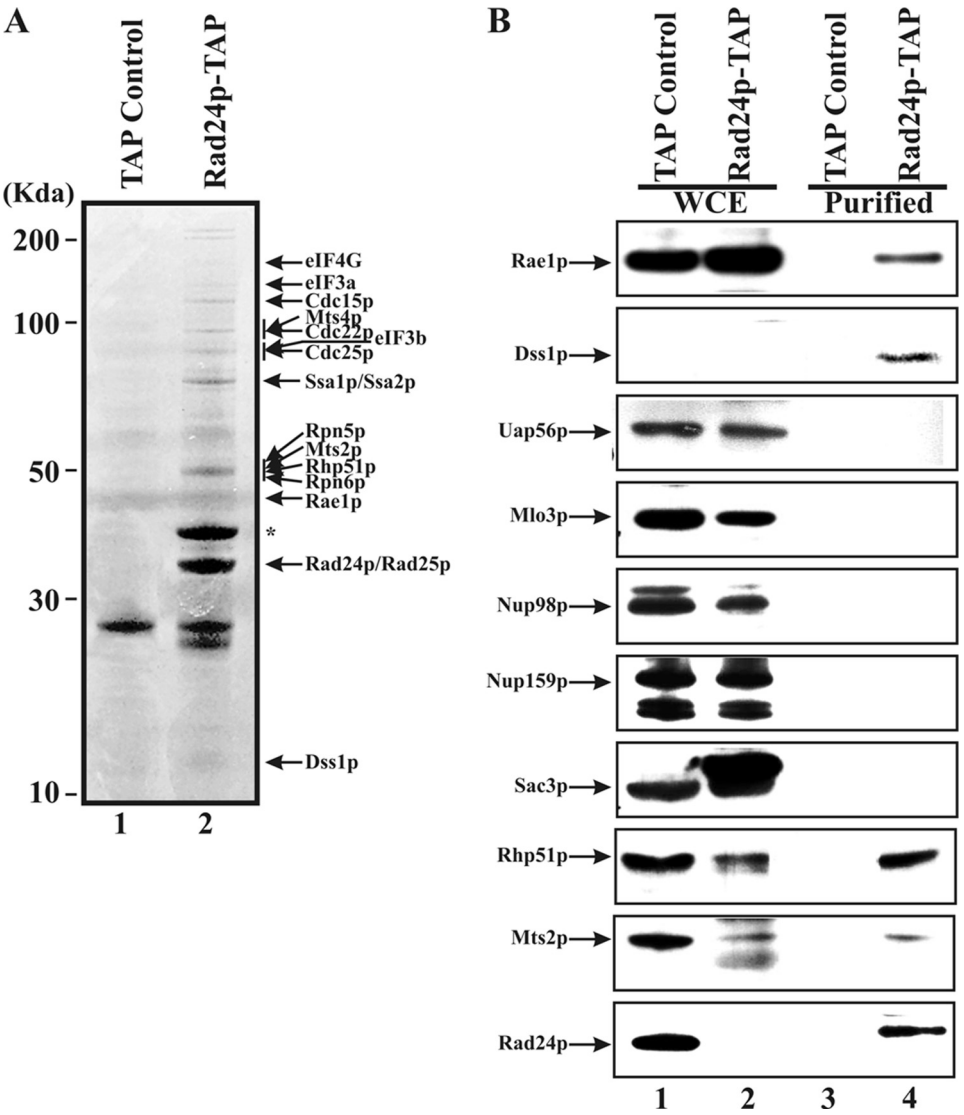

FIGURE 1. **Identification of Rad24p-TAP associated protein complex by tandem mass spectrometry and/or Western blot analysis.** *A*, tandem mass spectrometry analysis of Rad24p-TAP and their identified proteins are indicated (*lane 2*). The *asterisk* indicates the 60 ribosomal protein L2 (rpl402). *B*, input extracts from strains expressing TAP control or Rad24p-TAP fusion as indicated (*lanes 1* and *2*). TAP control or Rad24-TAP associated proteins purified on IgG-Sepharose and calmodulin beads as indicated (*lanes 3* and *4*). Proteins identified by specific antibodies are indicated. *WCE* represents whole cell extract. See "Experimental Procedures" for details.

amplification, PCR primers (Table 2) that did not amplify the precipitated products were used with each experiment as an internal control. [α-^{32}P]dCTP was added to the PCR. The amplified products were separated by electrophoresis on 6% Tris/borate/EDTA gel and quantified using phosphorimaging.

Chromatin Association Assay—The extracts were prepared from spheroplasts and nuclei according to published protocols (30, 41). The chromatin-associated fraction was separated from nuclear supernatant by layering the nuclear extract onto 30% sucrose cushion and centrifuged at 16,000 × *g* for 15 min (41). The chromatin-associated proteins were released by incubation with 277 units of DNase 1 for 10 min at 25 °C in a buffer containing 20 mM Hepes, pH 7.9, 1.5 mM magnesium acetate, 50 mM potassium acetate, 10% glycerol, 0.5 mM dithiothreitol, 150 mM Nacl, protease, and phosphatase inhibitors (42). Chromatin-associated protein was identified by Western blot analysis.

Construction of Plasmids—The *rad24* gene was isolated from a genomic library. For expression in bacteria, the *rad24* gene was amplified and introduced into pGEX4T-3 (Amersham Biosciences) and pET14b (Novagen) to produce GST and His-tagged Rad24p, respectively. Similarly His-Rhp51p also made with pET14b. Construction of His-tagged fusions of Rae1p and Dss1p were described previously (5).

Sensitivity to DNA-damaging Agents—Sensitivity to UV light was determined by plating 750–1000 cells and irradiating with a Stratagene UV-Stratalinker 2400 at fixed energy levels. The cells were then incubated at 21 °C, and the number of colonies was scored after 5 days. Sensitivity of cells to other DNA-damaging agents was determined by incubating liquid cultures cells in 3 milliunits/ml bleomycin or 0.03% methyl methanesulfonate (MMS) or 15 mM hydroxyurea (HU) (43–45). In parallel, control cells were incubated similarly without the addition of any DNA-damaging agent. Following incubation of 500–700 cells on YES plates, the surviving colonies were counted after 5 days.

Checkpoint Analysis—The cells were synchronized by sedimentation through 7–30% lactose gradient and plated on YES medium (46). The G_2 cells were irradiated with 0, 50, 100, and 150 J/m^2 UV light in a Stratagene Stratalinker 2400. The control cells were plated on YES medium without exposure to UV radiation. The cells were then resuspended and incubated at 21 °C or at 27 °C. Samples were taken at the indicated times, fixed in methanol at −20 °C, mounted, stained with 4,6-diamidino-2-phenylindole and calcofluor, and visualized under a fluorescence microscope. The cells were judged to have passed mitosis if either nuclear division or septum formation occurred.

RESULTS

Dss1p and Interacting Components Co-purify with Rad24p-TAP Fusion Protein—An *S. pombe* strain was constructed in which *rad24* gene was replaced by a *rad24-tap* gene fusion. As a negative control, TAP was expressed in wild type cells from a plasmid (pNTAP41) under the control of the *nmt1* promoter. Fig. 1*A* shows a typical TAP-purification experiment using genomic Rad24p-Tap fusion. Compared with the Tap control (*left lane*), several distinct bands were visible when Rad24-TAP

fusion was used to pull down interacting proteins whose identities were established by tandem mass spectrometric analysis. Elongation factors (eIF4G, eIF3a, and eIF3b), cell cycle factors (Cdc15p, Cdc22p, Cdc25p, and Rad25p), and 19 S proteasomal subunits (Mts4p, Rpn5p, Mts2p, and Rpn6p) were pulled down by Rad24p-Tap. DNA repair protein Rhp51p, Dss1p, and mRNA export factor Rae1p also co-purified with Rad24p-Tap fusion. Additional proteins identified using mass spectrometry (not shown in the gel in Fig. 1*A*) are presented in the supplemental Table 1S.

It is notable that only two known mRNA export factors (Rae1p and Dss1p) co-purified with Rad24p-Tap fusion protein. Western blot analysis was used to confirm these results. Fig. 1*B* shows the Western blot confirming that Rae1p and Dss1p co-purified with Rad24p-TAP but not with TAP alone (compare *lane 4 versus lane 3*). However, no other known mRNA export factor such as Uap56p, Mlo3p, Nup98p, Nup159p, and Sac3p co-purified with Rad24p-TAP. The absence of interaction with any other known mRNA export factor by Rad24p suggests that its interaction with Rae1p and Dss1p may represent a new complex, distinct from an mRNA export-related protein complex of these two proteins we previously described (5). By Western analysis we also confirmed interaction between Rad24p and Mts2p and Rhp51p. These results suggest that Rad24p physically interacts with at least some components of the proteasomes and the DNA recombination-repair pathway.

Dss1p, Rhp51p, and Mts2p Are Recruited to an HO-endonuclease-induced DSB Site in S. pombe Cells—We wanted to test whether in *S. pombe* Dss1p was recruited to DSB sites similar to Sem1p/human Dss1p. For this purpose, we used an *S. pombe* strain carrying the *S. cerevisiae* HO-endonuclease site integrated within the *arg3* locus (obtained from Paul Russell) (29). A schematic of the 5.4-kb genomic region surrounding the HO-endonuclease cleavage site (~2.1 kb upstream to ~3.2 kb downstream) and specific regions/fragments 1–9 that were amplified by PCR are shown in Fig. 2*A* (for details see Fig. 2 legend and Table 2). The strain was transformed with a plasmid expressing HO-endonuclease in pJR1–41XH vector under the control of a thiamine repressible *nmt1* promoter. By ChIP, DNA-bound proteins were precipitated using anti-Dss1p, anti-Rhp51p, or anti-Mts2p antibody from *S. pombe* cells in the presence or absence of HO-endonuclease expression. Quantitative PCR was performed to amplify specific fragments (*bars 1–9* in Fig. 2*A*) corresponding to both sides of the HO-endonuclease site as well as from a nontranscribed internal control region (at a different chromosomal locus (24) from the immunoprecipitated DNA obtained by antibodies or prebleed sera. Relative fold enrichment of DNA was calculated by using established procedures following the formula shown in Fig. 2*B*. Based on this calculation, a protein was considered enriched at a region when the DNA fold increase value was above 1 (see details in Fig. 2*B* legend) (39).

We previously showed that Dss1p recruits to actively transcribed genes in wild type *S. pombe* cells (5). In the absence of HO-endonuclease (control), in the *S. pombe* strain carrying the HO site, Dss1p showed a relative fold enrichment above 1 throughout the tested region (that also carried a functional kanamycin gene) (Fig. 2*C*, *panel a data* and *gray bars* in *graph*). In the cells expressing HO-endonuclease, Dss1p showed a clear pattern of enrichment around the break site. Enrichment was highest near the break site (peak relative enrichment ~5-fold proximal to the HO site; fragments 4–7) and gradually decreased away from the break site (fragments 1, 2, 3, 8, and 9).

Rad51p is known to recruit to DSB site in *S. cerevisiae*. We therefore tested whether Rhp51p similarly enriched at or around DNA break sites in *S. pombe*. Following a similar experimental procedure, we found that Rhp51p did not enrich within the test region in the control experiment (Fig. 2*C*, *panel b*, *gray bars* in *graph*). However, in the cells expressing the HO-endonuclease, there was significant increase in relative fold enrichment of the protein throughout the region (relative enrichment between 3–5-fold; fragments 1–9). Thus, in contrast to Dss1p, the pattern of enrichment shown by Rhp51p was different; it had an elevated level of enrichment both near and away from the break site, perhaps reflecting its nature of interaction with DNA.

Proteasomal components are known to recruit to DSB sites. We tested for the recruitment of Mts2p, a component of the proteasomes, to the DSB site. Mts2p was not significantly enriched in cells that did not express the HO-endonuclease (Fig. 2*C*, *panel c*, *gray bars* in *graph*). Relative fold enrichment of Mts2p was observed in the vicinity of the DSB site (highest enrichment, ~4.5-fold; Fig. 2*C*, *panel c*, *black bars* in *graph*, *fragments 3–7*) similar to the recruitment pattern observed for Dss1p in the strain expressing the HO-endonuclease. These results demonstrate that Dss1p, Rhp51p, and Mts2p are recruited preferentially surrounding the region of a DSB site introduced into the *S. pombe* cells, consistent with observations made with their homologs (12).

Rad24p and Rae1p Are Enriched at DSB Sites in S. pombe Cells—We previously showed that Rae1p was not recruited to active genes (5, 24). Also, it is not known whether Rad24 or any of its homologs recruit to genes. We wanted to test whether Rad24p and Rae1p were recruited to the DSB site in *S. pombe* cells. Following a similar experimental plan as above, we tested relative fold enrichment of Rad24p and Rae1p around the DSB site. Rad24p did not recruit efficiently within the 5.4-kb region in the cells not expressing the HO-endonuclease (Fig. 2*C*, *panel d*, control experiment). However, in presence of the HO-endonuclease, there was a significant relative fold enrichment of Rad24p with a pattern similar to Dss1p; there was maximum enrichment proximal to the break site (~5-fold) and a gradual decrease away from the break site in either direction (Fig. 2*C*, *panel d*, *black bars* in *graph*).

Finally, we tested for relative enrichment of Rae1p to the same 5.4-kb region in the presence or absence of the HO-endonuclease. Rae1p did not show preferential recruitment to any portion of the 5.4-kb region in cells not expressing the HO-endonuclease. However, in the cells expressing the HO-endonuclease, there was a significant relative fold enrichment of Rae1p around the DSB site (highest relative enrichment, ~4.5-fold; Fig. 2*C*, *panel e*, *black bars* in *graph*).

In a previous work, we showed that in *S. pombe* cells, Rae1p predominantly localizes at the nuclear pore (25). The current results are the first indication that some fraction of Rae1p could

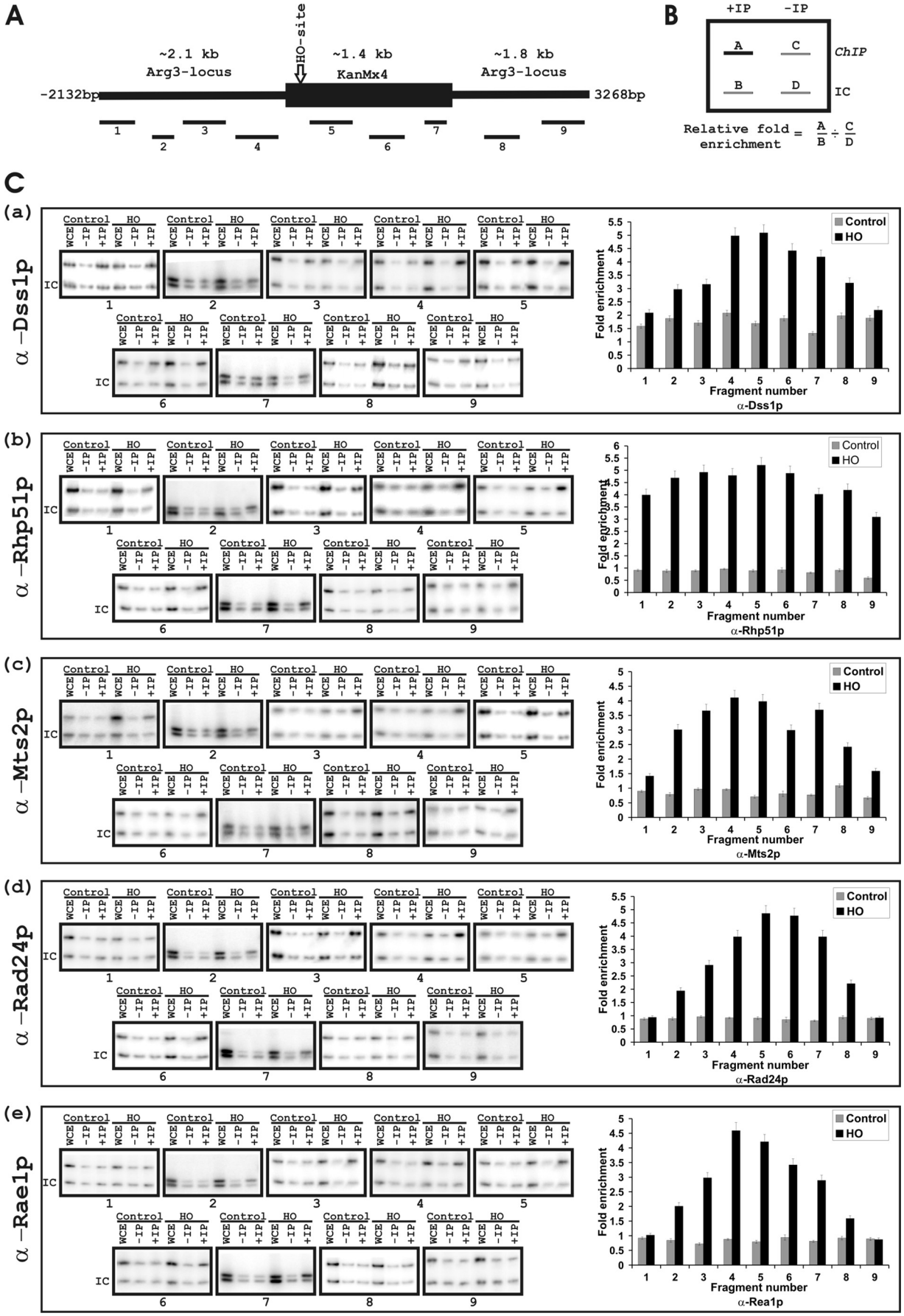
A
HO-site
~2.1 kb
Arg3-locus
~1.4 kb
KanMx4
~1.8 kb
Arg3-locus
-2132bp
3268bp
1
2
3
4
5
6
7
8
9
B
+IP
-IP
A
C
ChIP
B
D
IC
Relative fold enrichment = A/B ÷ C/D
C
(a)
α–Dss1p
(b)
α–Rhp51p
(c)
α–Mts2p
(d)
α–Rad24p
(e)
α–Rea1p
Control
HO
WCE
-IP
+IP
IC
Fold enrichment
Fragment number
α-Dss1p
α-Rhp51p
α-Mts2p
α-Rad24p
α-Rea1p

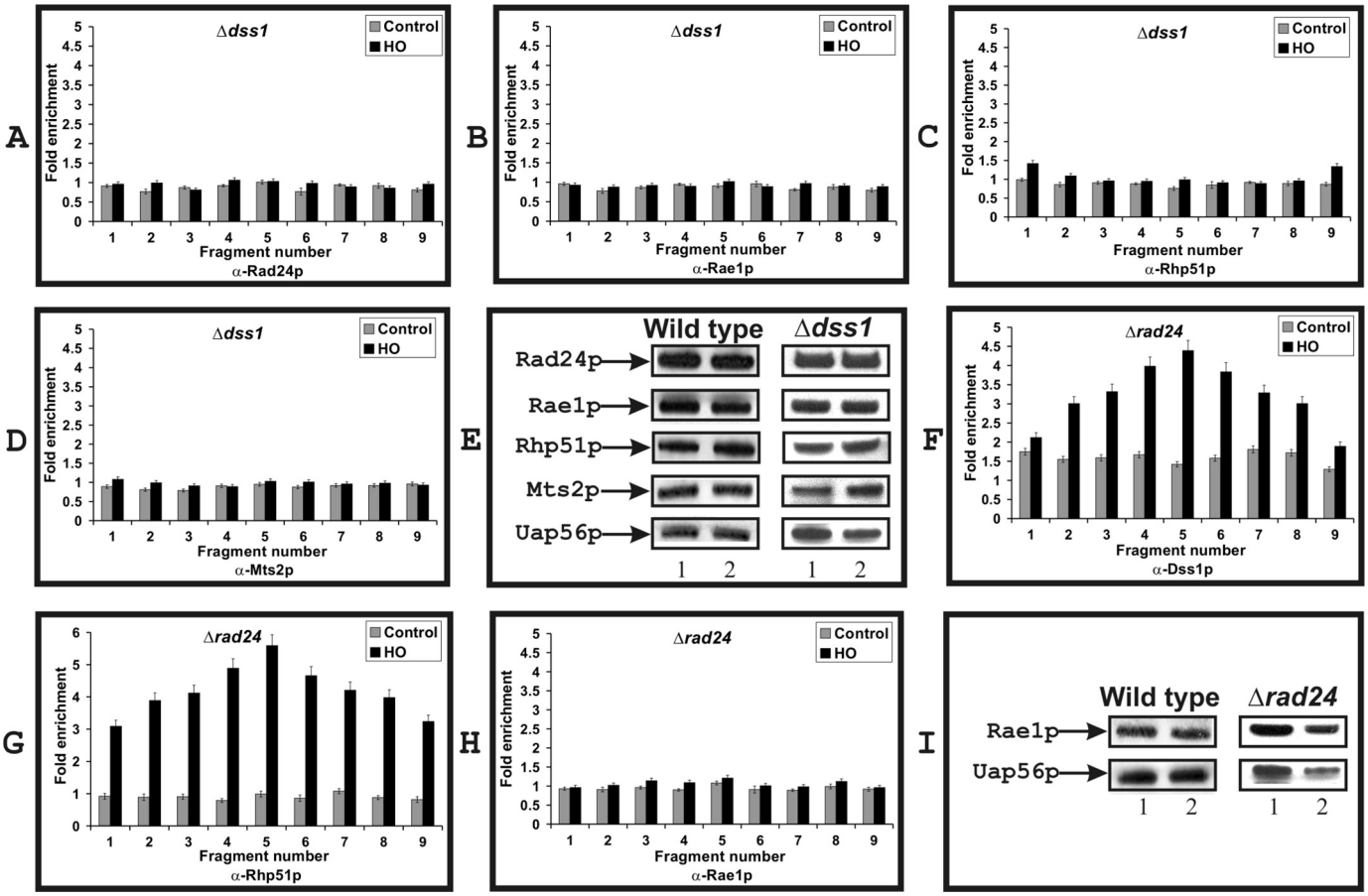

FIGURE 3. **Dss1p-dependent recruitment to the DSB site of proteins that co-purified with Rad24p-TAP.** *A–D* and *F–H*, as in Fig. 2*C*, graphical representations of the relative fold enrichment at each of the nine fragments are shown. Strain backgrounds and specific antibodies used in each experiment are indicated. See Fig. 2*C* for nomenclature and details of the experiments. The experimental data are provided as supplemental Fig. 1S. *E* and *I*, protein levels tested in wild type, Δ*dss1*, and Δ*rad24* strains. *Lane 1*, HO-endonuclease uninduced; *lane 2*, HO-endonuclease induced. Uap56p was used as an experimental control.

be physically (and functionally) associated with the genome. In addition, these results suggest that although under the normal cellular conditions Rad24p did not interact with the DNA region around the HO site, following DNA damage it was recruited to the DSB site similar to Dss1p, Rhp51p, Mts2p, and Rae1p. By considering the co-purification of proteins with Rad24p-TAP and the pattern of enrichment at the DSB site described above, it is likely that some of these proteins may function as a multiprotein complex(s) on DNA around the DSB site.

Dss1p Is Required for Recruitment of Rad24p, Rae1p, Rhp51p, and Mts2p to DSB Sites—We wanted to explore whether Dss1p-interacting proteins depended on Dss1p for their recruitment onto the DSB sites. In a Δ*dss1* strain, the recruitment of Rad24p, Rae1p, Rhp51p, and Mts2p was not detectable when HO-endonuclease was expressed (Fig. 3, *A–D*). We tested the amount of proteins present in the extract used for the ChIP experiment (shown in Fig. 3*E*) to rule out the possibility that lack of recruitment was not due to loss of proteins in the Δ*dss1* strain. As can be seen, the level of each protein in Δ*dss1* strain was comparable with the level observed in wild type cells (Fig. 3*E*). The lack of recruitment of all four proteins in the Δ*dss1* strain is strikingly different from the enrichment pattern observed in wild type cells (see Fig. 2*C* for comparison). These results strongly suggest that at the DSB site and the surrounding region, the recruitment of all four proteins depends on the presence of Dss1p.

In a Δ*rad24* strain, we found that the recruitment of Dss1p was unaffected, suggesting that Dss1p recruitment was independent of Rad24p (Fig. 3*F*, compare with Fig. 2*C*, *panel a*).

FIGURE 2. **Recruitment of *S. pombe* proteins to a genomic region containing a DSB site.** *A*, a schematic of the DNA fragment (5.4 kb) surrounding an HO-endonuclease cleavable site within a KanMX4 gene integrated into the *S. pombe* genome (29). Location and corresponding number represent different nonoverlapping regions surrounding the HO site whose amplification was tested by PCR. Primers used for PCR reaction are shown in Table 2. *B*, a schematic diagram showing the calculation for relative fold enrichment of proteins based on the formula shown (36). *IC* represents PCR product generated by using a pair of primers (Table 2) as internal control of the PCR reaction. *C*, *panels a–e*, individual ChIP experiment data shown on the *left*. Antibodies used for immunoprecipitation are as indicated. *WCE* is whole cell extract; *−IP*, prebleed sera was used for immunoprecipitation; *+IP*, antibodies as indicated were used for immunoprecipitation. *IC* is the internal control used in every experiment. Graphical representations of the quantification of relative/fold enrichment at each of the nine fragments are shown on the *right*. The *y* axis shows fold enrichment and *x*-axis shows each of the nine fragments tested and the corresponding antibodies used for the immunoprecipitation. Each *bar* is an average of three independent experiments. The *shaded bars* represent control experiments done in the absence of HO-endonuclease, and the *black bars* represent experiments performed in presence of the HO-endonuclease.

Similarly, Rhp51p was also enriched in Δ*rad24* strain at the DSB site similar to the pattern observed in the wild type cells (Fig. 3*G*, compare with Fig. 2*C*, *panel b*). Thus, Rhp51p was recruited independent of Rad24p. However, we found that Rae1p was not recruited significantly at the break site in a Δ*rad24* strain (Fig. 3*H*; see also supplemental Fig. 1S). Rae1p levels were tested in the Δ*rad24* strain, and no significant drop in the expression level of Rae1p in the Δ*rad24* strain was detected (Fig. 3*I*). These results indicate that (i) Dss1p is required for the recruitment of Rad24p, Rae1p, Rhp51p, and Mts2p to DSB sites and (ii) Rad24p is required for the recruitment of Rae1p.

Cdc25p Is Recruited to DSB Sites Dependent on Rad24p and Dss1p—The recruitment of Rad24p raised the interesting possibility that its interacting partner Cdc25p may associate with it and be recruited to DSB site upon DNA damage in *S. pombe* cells. To test this hypothesis, we constructed a wild type test strain carrying the HO-endonuclease cleavage site and a genomic copy of *cdc25-gfp* gene. Following the experimental plan as before, we tested the recruitment of Cdc25p-GFP in the presence or absence of HO-endonuclease in the strain. In the absence of the HO-endonuclease, there was no detectable enrichment of Cdc25p-GFP around the HO site (see control, *gray bars* in the histogram shown at the *right* of Fig. 4*A*, *panel a*). In contrast, there was a significant relative enrichment of Cdc25p-GFP around the DSB site when the HO-endonuclease expression was induced. These results clearly show that Cdc25p-GFP recruited to the DSB site in *S. pombe* cells during DNA damage.

To further explore how Cdc25p could be recruited to the DSB site, Cdc25p-GFP recruitment was tested in a Δ*rad24* strain. There was no detectable recruitment of Cdc25p-GFP in a Δ*rad24* strain with or without HO-endonuclease induction, demonstrating that there was no significant enrichment of Cdc25p-GFP to the DSB site (Fig. 4*A*, *panel b*). Thus, Cdc25p recruitment depended on Rad24p.

The activation of Chk1p is known to be required for Cdc25p-Rad24p interaction. To test whether Cdc25p-GFP recruitment was dependent on Chk1p, a Δ*chk1* strain carrying the HO site along with a genomic copy of Cdc25p-GFP was constructed. As can be seen in Fig. 4*A* (*panel c*), in the Δ*chk1* strain, Cdc25p-GFP did not recruit to the DSB site.

Cdc25p protein levels can vary within the cell at different time points in the cell cycle. So we wanted to exclude the possibility that loss of recruitment of Cdc25p-GFP was due to low levels of protein in the cell. Thus, we tested the relative amount of Cdc25p-GFP present in the wild type strain (carrying the HO site and genomic tagged Cdc25p-GFP) and in isogenic Δ*rad24* and Δ*chk1* strains before and after HO-endonuclease induction (Fig. 4*B*). Compared with the uninduced condition (*first*, *third*, and *fifth lanes*), under the induced condition (*second*, *fourth*, and *sixth lanes*) for the three strains, there was a significant increase in Cdc25p-GFP level as measured by detection of immunoprecipitated protein. The increase in the amount of Cdc25p-GFP in Δ*rad24* and Δ*chk1* cells (*fourth* and *sixth lanes*) is expected and is consistent with data from other observations (21) and suggests that the lack of recruitment of Cdc25p-GFP was not due to a low amount of the protein in the tested strains. These results are consistent with the suggested functional role of Chk1p kinase in Cdc25p-Rad24p interaction.

We finally tested whether the recruitment of Cdc25p-GFP to the DSB site depended on the presence of Dss1p. There was no detectable increase in the recruitment of Cdc25p-GFP to the HO site in the presence of HO-endonuclease in Δ*dss1* cells (Fig. 4*A*, *panel d*). We compared the relative amounts of Cdc25p-GFP protein under the HO-endonuclease induced and uninduced conditions. As expected there was a slight increase in the level of detectable Cdc25p-GFP in the HO-endonuclease-induced cells (Fig. 4*B*, compare *seventh* and *eighth lanes*). These results suggest that the lack of increase in the recruitment of Cdc25p-GFP to the DSB site in Δ*dss1* cells under the conditions of DNA damage was not due to the lack of available protein. Taken together, the recruitment of Cdc25p-GFP to the DSB site was dependent on the presence of Dss1p.

Following DSB, Cdc25p in the Nucleus Is Found Chromatin-associated—We next wanted to determine what fraction of nuclear Cdc25p-GFP is chromatin-associated following the formation of DSBs. We used the wild type strain carrying the HO-endonuclease cleavage site expressing *cdc25-gfp* to test the relative amounts of Cdc25p-GFP in total lysate (in Fig. 4*C*, *lanes T*; see figure legend for experimental details), total nuclear lysate (*TN*), nuclear supernatant (*NS*), and chromatin-associated fraction (*C*) in the presence and absence of the HO-endonuclease (Fig. 4*C*). In the absence of the HO-endonuclease, the nuclear Cdc25p-GFP was found to be present in the nuclear supernatant but not associated with the chromatin (compare *NS* and *C lanes* in the *Control panel*). In contrast, in cells expressing the HO-endonuclease, Cdc25p-GFP was detected in the chromatin-associated fraction but not in the nuclear supernatant (see *NS* and *C* in the *HO panel*). We used Uap56p, a nuclear protein, as a control to exclude the possibility that the lack of Cdc25p-GFP in the nuclear supernatant was not due to the absence of proteins in the extract. Fig. 4*C* shows that a comparable amount of nuclear supernatant protein was used in control and HO-endonuclease induced cells. These results indicate that in cells with DSB, all of the detectable nuclear Cdc25p is chromatin-associated.

We next investigated whether Cdc25p was also chromatin-associated in DNA damaged cells using ionizing radiation. The association of Cdc25p-GFP with chromatin was analyzed in asynchronous wild type cells expressing Cdc25p-GFP with and without γ radiation (300 grays) treatment (Fig. 4*D*). Following γ radiation chromatin was purified at 0, 1, 2, 3, and 4 h for determining its association with Cdc25p-GFP. Cdc25p-GFP was found to be associated with chromatin by 1, 2, and 3 h with maximum association at 2 h after treatment (Fig. 4*D*). α-Tubulin was used as an internal control for the total amount of protein loaded, and Coomassie staining of the gel was performed to show that proteins were present in samples that were chromatin-purified (Fig. 4*D*). These results indicate that Cdc25p is chromatin-associated even when cells are damaged using ionizing radiation.

Rad24p Directly Binds to Rae1p and Dss1p—Based on the ChIP experiments described above, one way that Rad24p could be recruited onto the DSB site was by direct physical interaction with Dss1p. Using proteins expressed and purified from *E. coli*

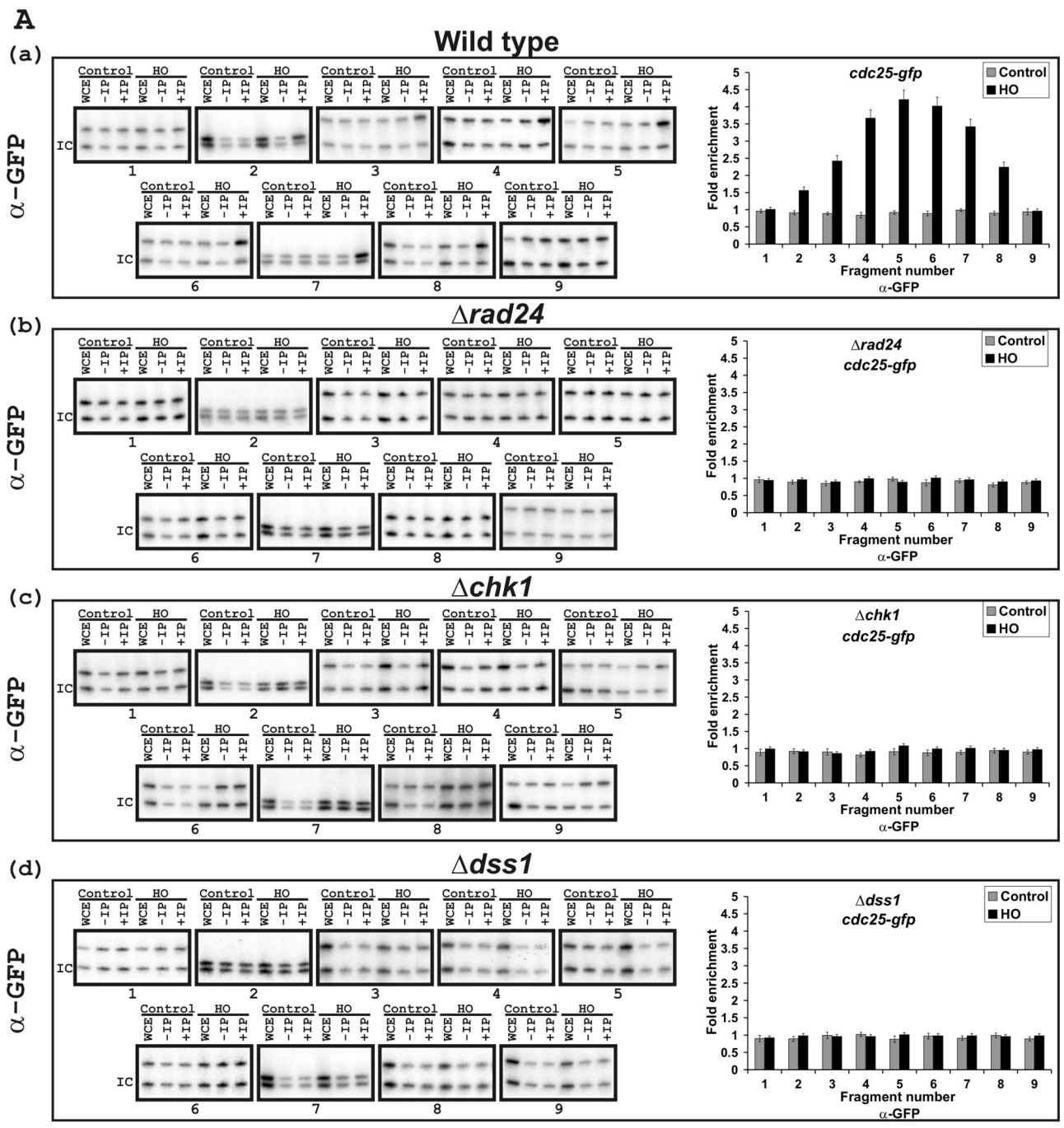
A
Wild type
(a)
α-GFP
Control
HO
WCE
-IP
+IP
IC
1
2
3
4
5
6
7
8
9
cdc25-gfp
Fold enrichment
Fragment number
α-GFP
Δrad24
(b)
Δrad24
cdc25-gfp
Δchk1
(c)
Δchk1
cdc25-gfp
Δdss1
(d)
Δdss1
cdc25-gfp
B
wild type
Δrad24
Δchk1
Δdss1
Cdc25p-GFP
Uap56p
C
Control
HO
T
TN
NS
C
Cdc25p-GFP
Uap56p
D
Total cell lysate
Chromatin associated
-IR
+IR
Hours
0
1
2
3
4
Cdc25p-GFP
Loading control

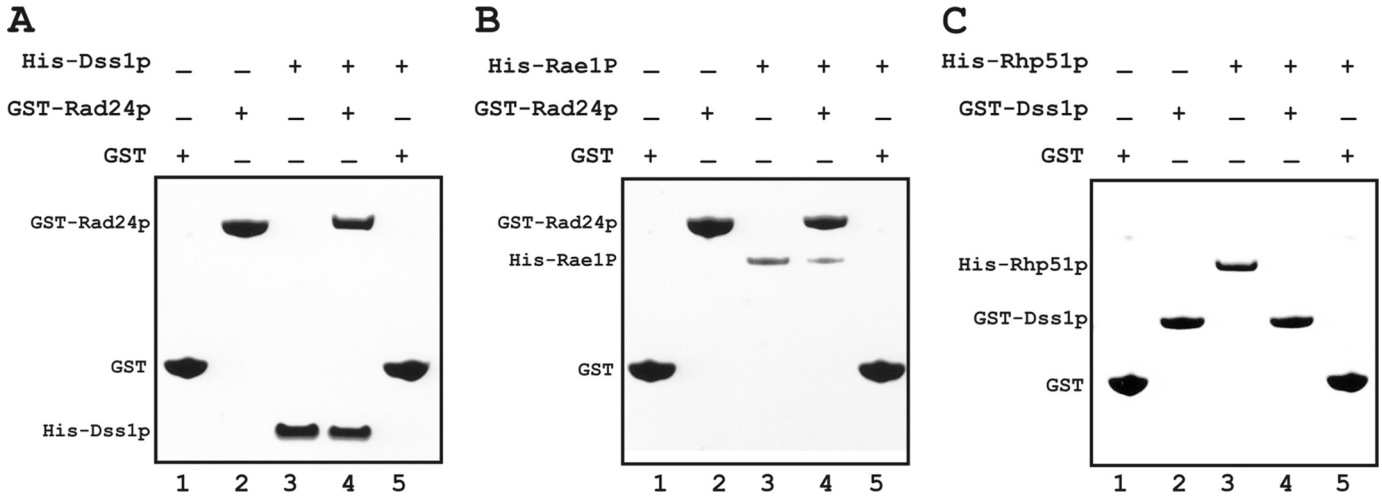

FIGURE 5. ***In vitro* binding of GST-Rad24p to His-Dss1p and His-Rae1p.** Proteins as indicated were made and purified from *E. coli* extracts. The presence or absence of a protein in the binding reaction is indicated by + or − on top of the respective lanes. Individual protein bands are shown. GST or GST-tagged proteins were immobilized on glutathione beads. *A*, binding of His-Dss1p by GST-Rad24p. *Lanes 1–3* are input. *Lane 4* is binding of His-Dss1p to GST-Rad24p on beads, and *lane 5* is binding of His-Dss1p to GST alone. *B*, binding of His-Rae1p by GST-Rad24p. *Lanes 1–3* are input. *Lane 4* is binding of His-Rae1p with GST-Rad24p, and *lane 5* is binding of His-Rae1p with GST. *C*, binding of His-Rhp51p by GST-Dss1p. *Lanes 1–3* are input. *Lane 4* is binding of His-Rhp51p with GST-Dss1p, and *lane 5* is binding of His-Rhp51p with GST alone. 5-fold more His-Dss1p, His-Rae1p, and His-Rhp51p over input was used in the binding reactions in *A*, *B*, and *C*, respectively. The bound proteins were analyzed by SDS-PAGE and Coomassie staining.

extracts, we tested direct interaction between Dss1p and Rad24p. Dss1p was able to bind GST-Rad24p fusion protein on beads but not GST alone (Fig. 5*A*, *lane 4 versus lane 5*).

The ChIP experiment also suggested that Rae1p recruitment was dependent on Rad24p. We therefore tested their interaction *in vitro*. GST-Rad24p, but not GST alone, was able to bind His-Rae1p (Fig. 5*B*, *lane 4 versus lane 5*). Because Rae1p recruitment onto DSBs depended on Rad24p (see previous section), these results clearly support the view that Rae1p-Rad24p interaction is essential for recruitment of Rae1p onto the DSB site, and Rad24p mediates Rae1p recruitment to DSB site. We previously showed direct physical interaction between Dss1p and Rae1p in a proposed messenger ribonucleoprotein complex critical for mRNA export (5). In contrast, here our results indicate that direct physical interaction with Dss1p does not determine recruitment of Rae1p.

Others have shown that homologs of Rhp51p associate with a Dss1p homolog indirectly within the recombination-repair complex (8, 9). Consistent with those studies, we detected no direct association between GST-Dss1p and His-Rhp51p (Fig. 5*C*, *lane 4*). Finally, direct physical interaction between Dss1p and Mts2p was not tested because their homologs are components of the 19 S proteasomal subcomplex and are known to interact with each other (12).

Dss1p Is Required for DNA Damage Checkpoint Function in S. pombe—We and others have shown that *dss1* mutants are sensitive to DNA-damaging agents such as UV light (5, 12). We wanted to test whether Δ*dss1* mutant cells were capable of activating the DNA damage checkpoint in response to UV light. As a control we used Δ*rad24* and wild type cells. Using a lactose gradient, we synchronized wild type, Δ*rad24*, and Δ*dss1* cells at G_2 stage. The G_2 synchronized cells were then exposed to varying doses of UV light, and the percentage of cells passing through mitosis over time at 27 °C was monitored and counted (Fig. 6*A*). Both Δ*dss1* and Δ*rad24* cells entered mitosis prematurely compared with the wild type cells. Strikingly, the timing of entry to mitosis by Δ*dss1* and Δ*rad24* cells was almost indistinguishable. One consequence of the Δ*dss1* cells entering mitosis prematurely was that the cells had abnormal morphologies (cut, anucleated, and multiseptated phenotypes) (Fig. 6*B*), similar to that seen for Δ*rad24* cells. These results indicate that Dss1p is required for monitoring DNA damage in the G_2 stage of the cell cycle.

rae1-1 Allele Is Sensitive to DNA-damaging Agents—Because Rae1p requires both Dss1p and Rad24p for recruitment to DSB site, we wanted to determine whether the *rae1* gene has any role in DNA damage in *S. pombe*. Wild type, *rae1-1*, Δ*rad24*, and *rae1-1* Δ*rad24* double mutant cells were treated with DNA-

FIGURE 4. **Recruitment of Cdc25p-GFP to a DSB-containing region.** *A*, *panels a–d*, extracts from cells expressing the integrated Cdc25p-GFP and HO-endonuclease site were used for immunoprecipitation using an anti-GFP polyclonal antibody. ChIP experiments were performed using wild type, Δ*rad24*, Δ*chk1*, and Δ*dss1* cells carrying integrated Cdc25p-GFP and an HO-endonuclease site. Experimental details and figure descriptions are as in Fig. 2. *B*, protein levels of Cdc25p-GFP in wild type, Δ*rad24*, Δ*chk1*, and Δ*dss1* cells. Equal amounts of proteins from various cell extracts were first immunoprecipitated by monoclonal antibodies to GFP, and following gel electrophoresis and Western blotting Cdc25p-GFP was detected by a polyclonal anti-GFP antibody (Clontech). Uap56p was used as an experimental control. *C*, chromatin association of Cdc25p-GFP was analyzed in the absence of HO-endonuclease (control) and in the presence of HO-endonuclease (*HO*) as shown. Total cell lysates (*T*), total nuclei (*TN*), nuclear supernatant (*NS*), and chromatin-associated fractions (*C*) were analyzed by Western blotting using anti-GFP polyclonal antibody (Clontech). The nuclear protein Uap56p was used as an experimental control. *D*, asynchronized wild type cells expressing the integrated Cdc25p-GFP were treated without (−*IR*) or 300-gray γ ionizing radiation (+*IR*). The samples were taken at indicated time intervals (h). Total cell lysate and chromatin-associated fractions were analyzed by Western blot using anti-GFP polyclonal antibody. As a loading control, anti-α-tubulin was used against total cell lysates, and Coomassie staining for chromatin-associated fractions was performed to show the presence of proteins.

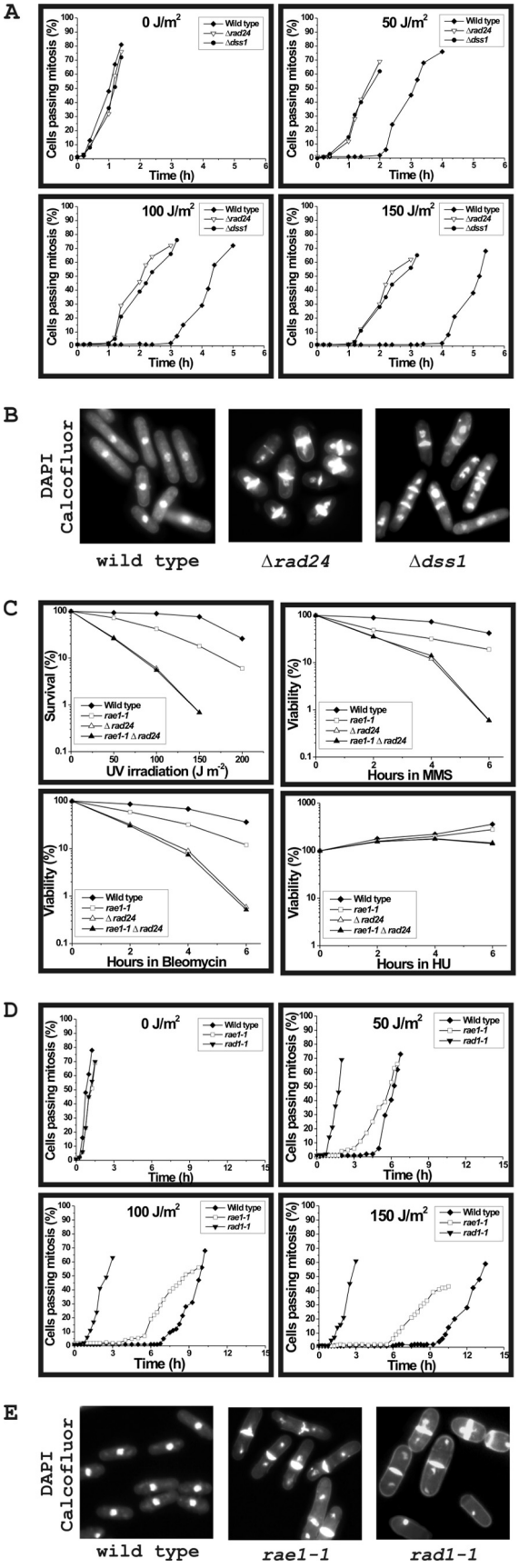

FIGURE 6. **Sensitivity to DNA-damaging agents and analysis of the checkpoint control of *S. pombe* wild type and mutant strains.** *A*, analysis of DNA damage checkpoint control in wild type, Δ*rad24*, and Δ*dss1* cells. G_2 synchronized cells were treated with different doses of UV light at 27 °C, and the cells were scored as having passed through mitosis if the nuclei had divided or septum had formed (see "Experimental Procedures" for details). *B*, morphology of cells treated with 4,6-diamidino-2-phenylindole (*DAPI*) and calcofluor following treatment with UV light with 100 J/m^2 when 20–25% of mutant cells had passed through mitosis. *C*, survival analysis at 21 °C of wild type, *rae1-1*, Δ*rad24*, and *rae1-1* Δ*rad24* treated with UV light, MMS, bleomycin, and HU as indicated (see "Experimental Procedures" for experimental details). *D*, analysis of checkpoint control in wild type, *rae1-1*, and *rad1-1* cells. See "Experimental Procedures" for details. The cells were scored as having passed through mitosis if the nucleus had divided or a septum had formed. *E*, morphology of cells following irradiation with UV light. When 20–25% of cells had passed through mitosis following irradiation with 100 J/m^2, the cells were fixed and stained with 4,6-diamidino-2-phenylindole and calcofluor. The morphology of wild type, *rae1-1*, and *rad1-1* cells is shown.

damaging agents such as UV light, bleomycin, MMS, and HU. Fig. 6*C* shows that wild type cells were not sensitive to any of the DNA-damaging agents. In contrast and as expected, Δ*rad24* cells were sensitive to UV, bleomycin, and MMS but not to HU. Similarly, *rae1-1* cells were sensitive to UV, MMS, and bleomycin and not to HU (Fig. 6*C*). The sensitivity of *rae1-1* cells was intermediate between wild type and Δ*rad24* mutant cells. The sensitivity of the *rae1-1* Δ*rad24* double mutant was similar to that of the more sensitive Δ*rad24* mutant cells, suggesting that in DNA damage, *rae1-1* mutation is epistatic to Δ*rad24*. Similar to Δ*rad24* mutant cells, *rae1-1* and the *rae1-1* Δ*rad24* double mutant also did not exhibit any sensitivity to HU, thus suggesting that Rae1p is unlikely to have a role in monitoring DNA damage during replication (Fig. 6*C*).

rae1-1 Mutation Shows Partial Loss of DNA Damage Checkpoint Function—Because the *rad24* gene is known to be involved in monitoring DNA damage in G_2, we tested whether *rae1-1* cells exposed to DNA-damaging agents such as UV light could fully activate the DNA damage checkpoint. Wild type, *rae1-1*, and *rad1-1* cells (*rad1* is a known DNA damage checkpoint gene) were synchronized in G_2 using a lactose gradient. These strains were exposed to varying doses of UV light, and the percentage of cells for each culture passing through mitosis over time was determined (Fig. 6*D*). In contrast to *rad1-1* cells, which showed essentially no arrest following treatment with UV light, *rae1-1* cells showed an initial checkpoint arrest but entered mitosis prematurely when compared with wild type cells. For example, following treatment with 150 J/m^2 of UV light, at 21 °C *rae1-1* mutant cells (these cells are temperature-sensitive at 25 °C) began to enter mitosis after a delay of 5 h as compared with 9 h for wild type cells (Fig. 6*D*).

The consequence of premature entry of *rae1-1* cells into mitosis was the generation of cells with abnormal morphologies. At 6.5 h following exposure to 100 J/m^2 of UV light, approximately 22% of the *rae1-1* cells had passed through mitosis, whereas less than 1% of wild type had done so. Of these, ~25% of *rae1-1* cells and 40% of *rad1-1* cells displayed either a cut or anucleated phenotype (Fig. 6*E*). These results suggest that *rae1-1* cells pass through mitosis prior to completely repairing their DNA and that Rae1p has a role in monitoring DNA damage in G_2.

DISCUSSION

In this work, we show that Dss1p has a DNA damage checkpoint function in *S. pombe* at the G_2/M boundary and functions

by recruiting the checkpoint protein Rad24p, cell cycle protein Cdc25p, and mRNA export/cell cycle factor Rae1p to DSB sites. To our knowledge, this is the first evidence of recruitment of these proteins to the damaged DNA sites, linking their functions in DNA damage and checkpoint via Dss1p. The similarity of timing and premature entry into mitosis by Δ*dss1* cells and Δ*rad24* cells suggests an epistatic relationship. This relationship is further revealed by direct physical interaction between Rad24p and Dss1p, placing them functionally together in DNA damage response. We further show that following DNA damage the nuclear Cdc25p is chromatin-associated. Finally, we propose that the recruitment of Cdc25p onto DSB site causes its intranuclear sequestration that could delay the timing of mitosis by arresting the cells at the G_2/M boundary in response to DNA damage.

Dss1p Is Critical for Linking DNA Repair and Checkpoint Functions in S. pombe Cells—ChIP experiments shed new light into how Dss1p functions in *S. pombe.* In this view, Dss1p is a key physical link between two functional complexes: one relating to DNA repair-recombination, and the other relating to the DNA damage checkpoint.

First, our results confirm observations made in other eukaryotic organisms about the physical association of Dss1p to DSB sites (8, 12). In addition, our data physically connect the recruitment of Rhp51p and Mts2p to DSB site through Dss1p.

Second, Dss1p is also essential for the recruitment of two additional proteins Rad24p and Rae1p. By examining the patterns of recruitment of Rad24p and Rae1p in wild type and Δ*dss1* backgrounds, a scheme of their recruitment on the DSB emerged. A simple sequential recruitment scheme (Dss1p < Rad24p < Rae1p) could explain the observed pattern. Proteins purified in *E. coli* allowed us to confirm direct physical interactions among Dss1p, Rad24p, and Rae1p. Consistently, we found evidence of direct physical interaction between Rad24p and Dss1p and between Rad24p and Rae1p. We could not directly investigate the formation of a ternary complex of Dss1p-Rad24p-Rae1p, because Dss1p and Rae1p also interact *in vitro* directly (5).

Recruitment of Rad24p to the DSB site raised the intriguing possibility of whether Cdc25p was also recruited by its interaction with Rad24p under the conditions of DNA damage. Indeed, a clear enrichment of Cdc25p following the pattern of Rad24p was discernible in the ChIP experiments. Cdc25p recruitment was also dependent on Dss1p. These results are consistent with Dss1p-mediated recruitment of Cdc25p via Rad24p into a single complex analogous to the Dss1p-Rad24p-Rae1p complex suggested above. Indeed, it is not unreasonable to speculate that a four protein complex of Dss1p, Rad24p, Rae1p, and Cdc25p may exist *in vivo* on or near DNA DSB sites.

Mechanism of Checkpoint Control in S. pombe Cells—In *S. pombe*, the Rad24p-Cdc25p interaction is well characterized in mediating G_2/M checkpoint control. The function of Rad24p is thought to be mediated by its binding to phosphorylated Cdc25p (47). Also, the binding of Rad24p to Cdc25p is preceded by activation and phosphorylation of Cdc25p by Chk1p kinase or independently by Mek1p (20, 47). Cdc25p dephosphorylates Cdc2p (47). It is thought that to establish G_2/M checkpoint control, Rad24p-Cdc25p complex exits the nucleus (nuclear exclusion), thereby physically removing the enzyme (Cdc25p) from its substrate (Cdc2p). However, recently it has also been suggested that nuclear exclusion of Cdc25p may not be essential for cell cycle arrest in response to DNA damage (22).

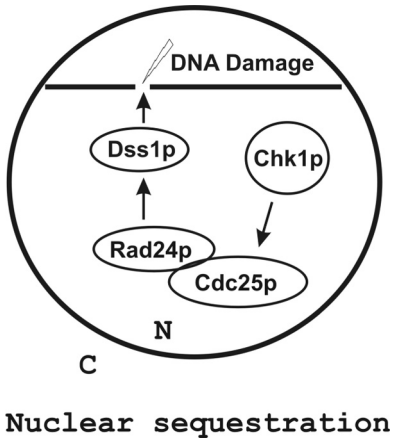

FIGURE 7. **Nuclear sequestration model of Cdc25p in response to DNA damage.** DNA damage leads to activation of Chk1p kinase that phosphorylates Cdc25p. Phosphorylated Cdc25p binds to Rad24p within the nucleoplasm (as shown in the schematic diagram) or after prebinding to DNA via Dss1p. In either case, Cdc25p is sequestered from its target Cdc2p.

Our results here support a new mechanistic scenario. In this scenario, DNA DSB formation signals activation of Chk1p kinase. At the DSB site, DNA repair factors including Dss1p are recruited (Fig. 7). Rad24p and Cdc25p (phosphorylated by activated Chk1p kinase) are recruited concurrently or sequentially to the break site via Dss1p. Rae1p is also likely recruited to the same site, dependent on Rad24p and Dss1p. The recruitment of Cdc25p physically separates it from its target Cdc2p and thus prevents it from activating Cdc2p. In the absence of active Cdc2p, the cells are prevented from entering mitosis. Once the DNA is repaired, the protein complexes are likely disassembled, releasing Cdc25p into the nucleoplasm to interact with and activate Cdc2p. This in turn allows the cells to enter mitosis.

What Is the Role of Rae1p in Checkpoint Control in S. pombe?—Several experiments now link Rae1p to the *S. pombe* cell cycle progression. First, *rae1-1* temperature sensitive mutant at the restrictive temperature causes cells to arrest at G_2/M boundary (25, 37). Sensitivity of *rae1-1* cells to DNA-damaging agents shown here is consistent with a functional role in monitoring DNA damage and/or cell cycle. Interestingly, another mutant of *rae1* (*rae1-167*) was not sensitive to any DNA-damaging agent (data not shown), suggesting allele specificity of the function of Rae1p in DNA damage. Second, we have previously shown the role of Rae1p in mRNA export within a protein complex comprised of mRNA export factors Uap56p, Dss1p, and Mlo3p. Most of the *S. pombe* Rae1p is localized to the nuclear pore in association with nucleoporin Nup98 (25). Our hypothesis is that a Rae1p-containing mRNA export complex functions at the nuclear pore. In contrast, the recruitment of Rae1p to the DSB site described in this paper is reflective of a separate protein complex with components that are not known to be linked to mRNA export. In particular, neither Nup98 nor Nup159 associated with the Rad24p-purified complex that pulled down Rae1p. (Rae1p is stably bound to Nup98 in mRNA export complexes, and these proteins co-purify *in vivo*/*in vitro*

(48)). Third, the direct physical interaction between Rae1p and Rad24p *in vitro* and Rad24p-dependent recruitment of Rae1p *in vivo* suggest a molecular basis for Rae1p function through Rad24p in checkpoint control. Finally, for establishing cell cycle delay, Cdc25p function must be inhibited so that it does not activate Cdc2p. The timing of the function of Rae1p in the cell cycle also places it prior to Cdc2p activation (23, 25). Based on the work described here, the key future question regarding the role of Rae1p in checkpoint control is whether its function affects Cdc2p directly or indirectly (*i.e.* via Cdc25p) or via another target protein.

Acknowledgments—We thank Dr. Paul Russell, Dr. Paul G. Young, and Dr. Kathleen L. Gould for providing strains and plasmids, lab members for helpful discussions, and Dr. Joseph Landry and National Institutes of Health Fellows Editorial Board members for reading and correcting the manuscript.

REFERENCES

1. Bucher, N., and Britten, C. D. (2008) *Br. J. Cancer* **98,** 523–528
2. Sancar, A., Lindsey-Boltz, L. A., Unsal-Kaçmaz, K., and Linn, S. (2004) *Annu. Rev. Biochem.* **73,** 39–85
3. Berry, L. D., and Gould, K. L. (1996) *Prog. Cell Cycle Res.* **2,** 99–105
4. Mannen, T., Andoh, T., and Tani, T. (2008) *Biochem. Biophys. Res. Commun.* **365,** 664–671
5. Thakurta, A. G., Gopal, G., Yoon, J. H., Kozak, L., and Dhar, R. (2005) *EMBO J.* **24,** 2512–2523
6. Yang, H., Jeffrey, P. D., Miller, J., Kinnucan, E., Sun, Y., Thoma, N. H., Zheng, N., Chen, P. L., Lee, W. H., and Pavletich, N. P. (2002) *Science* **297,** 1837–1848
7. Zhou, Q., Kojic, M., Cao, Z., Lisby, M., Mazloum, N. A., and Holloman, W. K. (2007) *Mol. Cell. Biol.* **27,** 2512–2526
8. Gudmundsdottir, K., Lord, C. J., Witt, E., Tutt, A. N., and Ashworth, A. (2004) *EMBO Rep.* **5,** 989–993
9. Kojic, M., Yang, H., Kostrub, C. F., Pavletich, N. P., and Holloman, W. K. (2003) *Mol. Cell* **12,** 1043–1049
10. Jang, Y. K., Jin, Y. H., Shim, Y. S., Kim, M. J., Yoo, E. J., Choi, I. S., Lee, J. S., Seong, R. H., Hong, S. H., and Park, S. D. (1996) *Mol. Gen. Genet.* **251,** 167–175
11. Muris, D. F., Vreeken, K., Carr, A. M., Broughton, B. C., Lehmann, A. R., Lohman, P. H., and Pastink, A. (1993) *Nucleic Acids Res.* **21,** 4586–4591
12. Krogan, N. J., Lam, M. H., Fillingham, J., Keogh, M. C., Gebbia, M., Li, J., Datta, N., Cagney, G., Buratowski, S., Emili, A., and Greenblatt, J. F. (2004) *Mol. Cell* **16,** 1027–1034
13. Funakoshi, M., Li, X., Velichutina, I., Hochstrasser, M., and Kobayashi, H. (2004) *J. Cell Sci.* **117,** 6447–6454
14. Jossé, L., Harley, M. E., Pires, I. M., and Hughes, D. A. (2006) *Biochem. J.* **393,** 303–309
15. Bruckmann, A., Steensma, H. Y., Teixeira De Mattos, M. J., and Van Heusden, G. P. (2004) *Biochem. J.* **382,** 867–875
16. Hermeking, H., and Benzinger, A. (2006) *Semin. Cancer Biol.* **16,** 183–192
17. van Heusden, G. P. (2005) *IUBMB Life* **57,** 623–629
18. van Heusden, G. P., and Steensma, H. Y. (2006) *Yeast* **23,** 159–171
19. Ford, J. C., al-Khodairy, F., Fotou, E., Sheldrick, K. S., Griffiths, D. J., and Carr, A. M. (1994) *Science* **265,** 533–535
20. Pérez-Hidalgo, L., Moreno, S., and San-Segundo, P. A. (2008) *Cell Cycle* **7,** 3720–3730
21. Lopez-Girona, A., Furnari, B., Mondesert, O., and Russell, P. (1999) *Nature* **397,** 172–175
22. Lopez-Girona, A., Kanoh, J., and Russell, P. (2001) *Curr. Biol.* **11,** 50–54
23. Brown, J. A., Bharathi, A., Ghosh, A., Whalen, W., Fitzgerald, E., and Dhar, R. (1995) *J. Biol. Chem.* **270,** 7411–7419
24. Thakurta, A. G., Selvanathan, S. P., Patterson, A. D., Gopal, G., and Dhar, R. (2007) *J. Biol. Chem.* **282,** 17507–17516
25. Whalen, W. A., Bharathi, A., Danielewicz, D., and Dhar, R. (1997) *Yeast* **13,** 1167–1179
26. Blower, M. D., Nachury, M., Heald, R., and Weis, K. (2005) *Cell* **121,** 223–234
27. Jeganathan, K. B., Malureanu, L., and van Deursen, J. M. (2005) *Nature* **438,** 1036–1039
28. Wong, R. W., Blobel, G., and Coutavas, E. (2006) *Proc. Natl. Acad. Sci. U.S.A.* **103,** 19783–19787
29. Du, L. L., Nakamura, T. M., Moser, B. A., and Russell, P. (2003) *Mol. Cell. Biol.* **23,** 6150–6158
30. Alfa, C., Fantes, P., Hyams, J., Mcleod, M., and Warbrick, E. (1993) *Experiments with Fission Yeast*, Cold Spring Harbor Press, Cold Spring Harbor, NY
31. Moreno, S., Klar A., and Nurse, P. (1991) *Methods Enzymol.* **194,** 795–823
32. Bähler, J., Wu, J. Q., Longtine, M. S., Shah, N. G., McKenzie, A., 3rd, Steever, A. B., Wach, A., Philippsen, P., and Pringle, J. R. (1998) *Yeast* **14,** 943–951
33. Rigaut, G., Shevchenko, A., Rutz, B., Wilm, M., Mann, M., and Séraphin, B. (1999) *Nat. Biotechnol.* **17,** 1030–1032
34. Puig, O., Caspary, F., Rigaut, G., Rutz, B., Bouveret, E., Bragado-Nilsson, E., Wilm, M., and Séraphin, B. (2001) *Methods* **24,** 218–229
35. Ilani, T., Khanna, C., Zhou, M., Veenstra, T. D., and Bretscher, A. (2007) *J. Cell Biol.* **179,** 733–746
36. Simkus, C., Bhattacharyya, A., Zhou, M., Veenstra, T. D., and Jones, J. M. (2009) *Immunology* **128,** 206–217
37. Bharathi, A., Ghosh, A., Whalen, W. A., Yoon, J. H., Pu, R., Dasso, M., and Dhar, R. (1997) *Gene* **198,** 251–258
38. Yoon, J. H., Love, D. C., Guhathakurta, A., Hanover, J. A., and Dhar, R. (2000) *Mol. Cell. Biol.* **20,** 8767–8782
39. Noma, K., Allis, C. D., and Grewal, S. I. (2001) *Science* **293,** 1150–1155
40. Partridge, J. F., Borgstrøm, B., and Allshire, R. C. (2000) *Genes Dev.* **14,** 783–791
41. Lygerou, Z., and Nurse, P. (1999) *J. Cell Sci.* **112,** 3703–3712
42. Nishitani, H., Lygerou, Z., Nishimoto, T., and Nurse, P. (2000) *Nature* **404,** 625–628
43. Enoch, T., Carr, A. M., and Nurse, P. (1992) *Genes Dev.* **6,** 2035–2046
44. Morishita, T., Tsutsui, Y., Iwasaki, H., and Shinagawa, H. (2002) *Mol. Cell. Biol.* **22,** 3537–3548
45. Rhind, N., and Russell, P. (2001) *Mol. Cell. Biol.* **21,** 1499–1508
46. Barbet, N. C., and Carr, A. M. (1993) *Nature* **364,** 824–827
47. Russell, P. (1998) *Trends Biochem. Sci.* **23,** 399–402
48. Blevins, M. B., Smith, A. M., Phillips, E. M., and Powers, M. A. (2003) *J. Biol. Chem.* **278,** 20979–20988
49. Rowley, R., Subramani, S., and Young, P. G. (1992) *EMBO J.* **11,** 1335–1342
50. Chua, G., Lingner, C., Frazer, C., and Young, P. G. (2002) *Genetics* **162,** 689–703
51. Roguev, A., Shevchenko, A., Schaft, D., Thomas, H., Stewart, A. F., and Shevchenko, A. (2004) *Mol. Cell Proteomics* **3,** 125–132